Trop J Nat Prod Res, July 2021; 5(7):1271-1277 ISSN 2616-0684 (Print)
ISSN 2616-0692 (Electronic)

Tropical Journal of Natural Product Research

Available online at https://www.tjnpr.org

Original Research Article

Adsorption and Inhibitory Properties of *Buchholzia coriacea* Seed Extracts on Mild Steel Corrosion in Acidic Media

Christogonus O. Akalezi[1,2]*, Nwanneamaka R. Oze[1], Emeka E. Oguzie[1,2]

[1]*Electrochemical and Material Science Unit (EMRU), Department of Chemistry, Federal University of Technology Owerri, PMB 1526 Owerri, Nigeria*
[2]*African Center of Excellence in Future Energies and Electrochemical Systems, Federal University of Technology Owerri, PMB 1526 Owerri, Nigeria*

ARTICLE INFO

Article history:
Received 03 January 2021
Revised 28 May 2021
Accepted 07 July 2021
Published online 02 August 2021

ABSTRACT

Corrosion inhibitors can be defined as substances that are added in small amounts to the environment preventing metal from further degradation. While choosing the inhibitor several factors such as its cost, toxicity, availability and environment friendliness need to be taken into account. Despite the high efficiency of many commonly used synthetic compounds, they are often toxic, carcinogenic or even allergenic. Thus, there has been emerging need to search for cost effective and more environmentally friendly corrosion inhibitors obtained from renewable resources. This study was designed to investigate the application of *Bucholzea coriacea* seed (BCS) extract as a potential inhibitor for mild steel corrosion in acidic media. Use of GC/MS study on the crude extract enabled identification of eight major constituents, namely 4,5-Dihydro-2-methyl imidazole-4-one (DMM), 4,6-Dimethyltetrahydro-2H-pyran-2-one (DTP), 1-Methyl-pyrrolidine-2-carboxylic acid (MPC),2-Pyrrolidinoethylamine (PEA), (4E)-4-Methyl-4-heptane-3-one (MHT), Nitroisobutyl glycerol (NBG), 1,4-Dimethoxy-2-methylcyclohexane (DMH), 1-Pentadecanecarboxylic acid (PCA). The identified structures were studied using Molecular Dynamics (MD) simulation in a Dmol3 module available in Material Studio (MS 4.0). Key structural parameters including the energies of the highest occupied molecular orbital (HOMO) and lowest unoccupied molecular orbital (LUMO), energy gap (ΔE) and the dipole moment were calculated and discussed. The thermodynamic functions of dissolution and adsorption processes were calculated from gravimetric data and the interpretation of the results are given. The adsorption of this plant extract on the mild steel surface obeys the Langmuir adsorption isotherm.

Keywords: *Bucholzea coriacea*; Inhibitor; Adsorption isotherm; Molecular modeling.

Introduction

Many corrosion control methods are applicable for the protection of metallic structures under exposure in various corrosive environments. The use of corrosion inhibitors is one of the most effective alternatives especially in areas where the electrolyte solution is of a known and controllable quantity such as oil well acidizing, industrial washings, acid de-scaling.[1] On ships, this occurs onboard equipment (boilers tanks, pipes etc.). Corrosion inhibitors whether organic or inorganic retard the corrosion rate by affecting the two elements of the corrosion process. Anodic inhibitors work by migrating to the anode and react to form salts which act as protective barriers. Examples are chromates, nitrites, phosphates and soluble oils. Cathodic inhibitors either inhibit oxygen absorption or hydrogen evolution. Examples are salts of magnesium, zinc, nickel or arsenic compounds. Organic compounds bearing heteroatoms with high electron density such as phosphor, sulfur, nitrogen, oxygen or those containing multiple bonds which are considered as adsorption centers, are effective as corrosion inhibitor. The existing data show that organic inhibitors act by adsorption and protect the metal by film formation.

*Corresponding author. E mail: chrisakalezi@yahoo.com
Tel: +2348080587128

Citation: Akalezi CO, Oze NR, Oguzie EE. Adsorption and Inhibitory Properties of *Buchholzia coriacea* Seed Extracts on Mild Steel Corrosion in Acidic Media. Trop J Nat Prod Res. 2021; 5(7):1271-1277. doi.org/10.26538/tjnpr/v5i7.19

Official Journal of Natural Product Research Group, Faculty of Pharmacy, University of Benin, Benin City, Nigeria.

However, due to increasing awareness of the toxic properties of most organic corrosion inhibitor compounds in current use, and the accompanying ecological and health risks, researchers are moving towards exploring more environmentally friendly inhibitor sources.[2-6] Available data, points towards plant extracts as the most acceptable candidate in this transition. Plants extracts are not only environmentally safe and available; they are equally effective under a wide range of corrosion environments having similar chemical composition with conventional corrosion inhibitors.[7-14]

Despite the sustained interest in the use of organic extracts for corrosion protection, a major challenge has been that of deducing the detailed mechanisms of the inhibition process and determining the individual contributions of the many constituents to the total inhibiting effect of the extracts. The intricate chemical compositions of the extracts, makes it difficult to allocate the inhibition activity to any specific constituent. A novel approach developed by Oguzie and Co-Workers (2010)[15] involves evaluation of the elucidated molecular structures of the phytochemical constituents of the extracts by computer simulations of suitable models based on the Density Functional Theory (DFT). This enables theoretical assessment of corrosion inhibiting potential based on certain structure-activity relationships (SAR) to estimate basic quantum chemical/molecular descriptors identifiable with corrosion inhibition performance.

Buchholzia coriacea, belonging to the family Capparidaceae is an evergreen, small to medium-sized tree growing up to 20 m tall commonly found in the rain forest zones of Africa especially Cameroon, Central African Republic, Gabon, Congo, Angola, Ghana, Nigeria, among others.

The fruits of *Buchholzia coriacea* are oval, resembling avocado pears, with a thick and woody endocarp, yellowish when ripe; containing a

few large blackish seeds.[16--21] The name, wonderful kola) is derived from the seed arising from its popular usage in traditional medicine. The phytochemical screening of dried seeds of *Buchholzia coriacea* reveals the presence of alkaloids, glycosides, saponin, steroids, tannin, flavonoids, terpenes, reducing sugars and phenol from ethanol extract. However, there has been no previous use of this plant for corrosion inhibition purposes. The focus of the present study is to investigate the potentials of BCS extract as a corrosion inhibitor of mild steel in corrosive solutions. The assessment of the corrosion behavior of the major constituents in the extract was studied using molecular modeling to calculate the molecular properties most relevant to their inhibitory activity. The electronic properties calculated include the highest occupied molecular orbital (HOMO) and the lowest unoccupied molecular orbital (LUMO) energy levels, the energy gap (ΔE), and the dipole moments. Other properties evaluated include ionization potential, electronegativity, hardness and softness. These parameters give valuable information about the reactivity behavior of a compound

Materials and Methods

Collection and authentication of plant material
Fruits of *Bucholzea coreacea* were collected from a village in Amuzi in Ahiazu-Mbaise LGA (Imo State) during the month of December, 2019. The seeds were authenticated by a taxonomist in the department of Crop Science Federal University of Technology Owerri, Imo State. The voucher number of the specimen deposited is CST/BC-010102. The fruits were taken to our laboratory where they were dehulled, sun dried and kept in desiccators until needed.

Materials and reagents preparation
Sun-dried pulverized *Bucholzea coreacea* seeds (80 g) were extracted in 250 mL boiling ethanol for 6 hours. The extracts were cooled, filtered, and concentrated by evaporating the excess solvent. The solid products obtained were reconstituted with ethanol to the appropriate concentrations as required for the GC/MS and corrosion inhibition studies. All reagents were of analytical grade and obtained from (Merck) India. The aggressive solutions (1 M HCl) were prepared by dilution of an analytical reagent grade 37 % HCl with doubly distilled water. Mild steel sample having the following composition 0.189% C, 0.145% Si, 0.429% Mn, 0.223% Cu, 0.043% S and Fe balance and cut to dimensions of 3 x 3 x 0.15 cm were the coupons. Three grades of emery papers applied in turn enabled a smooth metal surface using ethanol to degrease.

Weight loss measurements
The concentration range of the BCS extract used was varied from 50 to 1000 mg/L and the electrolyte used was 200 mL for each experiment at 303K. However, during the test at higher temperatures (T>303K) only two concentrations (50 and 1000 mg/L) were considered. The metal coupons were accurately weighed after degreasing with acetone. The immersion times were 24 h for test at 303 K and 3 h for tests at the higher temperatures. The metal coupons were retrieved after the appropriate corroding time, scrubbed with a bristle brush, then dried and reweighed. The data reported were the average of triplicate runs
The inhibition efficiency IE% was calculated using the following equation: [15]

$$IE\% = \frac{w_o - w_i}{w_i} x100 \quad (1)$$

Where w_i and $W0$ are the weight loss of the mild steel in the presence and absence of extract additive, respectively.

Gas chromatography-mass spectrometry (GC–MS)
About 10 µL BCS extract sonicated with ethanol were analyzed by GC–MS using Shimadzu Model GCMS-QP2010 PLUS equipped with flame ionization detection (FID) and a CBP-5 capillary fused silica column (25 m, 0.25 mm i.d., 0.22 µm film thickness). The oven temperature was set at 50^{o}C and held for 2 min, then programmed at 10^{o}C/min to 250^{o}C, and finally held for 20 min. The carrier gas is He (99.99%) let in at a pressure of 76 kPa, with a linear velocity of 20 cm/s and split ratio, 1:25; injector and detector temperatures were 250^{o}C and 310^{o}C respectively.

Computational study
Molecular modeling calculation was accomplished in the Dmol3 module available in Material Studio (MS) software from Accelrys Inc.[22-24] using an optimization procedure incorporating a COMPASS force field, a Perdew-Wang (PW) functional [25] a double numeric quality basis set (DND) and a smart minimization method with high convergence. The distribution of frontier molecular orbitals including the highest occupied molecular orbital (HOMO) and the lowest unoccupied molecular orbital (LUMO) were obtained from this optimized structure. The calculations and analysis were in the vacuum phase.

Results and Discussion

Analysis of plant extract
GC-MS chromatogram of the ethanol extracts of *Buchholzia coriacea* seeds showed eight prominent peaks as shown in Figure 1. The eight active constituents with their retention time (RT), molecular formula, molecular weight (MW) and peak area (%) in the ethanol extract of *Buchholzia coriacea* seeds are presented in Table 1. The identity of the components in the extract assigned by the comparison of their retention indices and mass spectra fragmentation patterns with those stored on the computer library, also with the published literature. Table 2 show the structures of the compounds obtained.

Computational results
Quantum chemical calculations
Figure 2 presents the optimized structures of the eight BCS components; the HOMO and LUMO molecular orbitals. According to the frontier molecular orbital theory of chemical reactivity, transition of electron is due to an interaction between the frontier orbitals highest occupied molecular orbital (HOMO) and lowest unoccupied molecular orbital (LUMO) of reacting species. Table 3 reports the calculated total energies of the compounds, E_{HOMO} and E_{LUMO} orbital energies and energy gaps, $\Delta E_{LUMO-HOMO}$ and dipole moments, µ obtained by Dmol3 calculations.
The HOMO energy can indicate the disposition of the molecule to donate electrons to an appropriate acceptor with empty molecular orbital. In addition, an increase in the values of E_{HOMO} (Less negative) can facilitate the adsorption and therefore higher inhibition efficiency.[26] LUMO energy (E_{LUMO}), on the other hand, indicates the ability of the molecule to accept electrons; therefore, inhibition efficiency increases with decreasing LUMO energy of the inhibitors. The order of increasing values of E_{HOMO} and decreasing the E_{LUMO}, according this study is: MHT< MPC< NBG< DMM & PEA<DTP<PCA<DMH. Excellent corrosion inhibitors are usually those organic compounds, which do not only offer electrons to unoccupied orbital of the metal, but also accept free electrons from the metal. [24] Therefore, for a given molecule, the lower values of E_{LUMO}, the greater its capability to accept electrons such as 4s electrons from Fe.[32-35] The obtained values of E_{HOMO} corresponding to each of the organic inhibitors under study have only small difference between them. This indicates a very similar capacity for charge donation to the metallic surface.[27, 28] The corrosion rate must decrease with increase in HOMO energy; therefore, an increase in the corrosion inhibition is present. Low values of the gap energy (ΔE) will provide good inhibition efficiencies, because the excitation energy to remove an electron from the last occupied orbital will be below. Dipole moment µ is the measure of polarity in a bond and relates to the distribution of electrons in a molecule, and predicts the direction of a corrosion inhibition process. In spite of the fact that literature is conflicting on the utilization of µ as an indicator of the direction of a corrosion inhibition reaction, it is for the most part concurred that the adsorption of polar compounds having high dipole moments on the metal surface ought to prompt better inhibition efficiency.[28-33] This being the case, the dipole moment values presented in Table 3 will reflect the

ISSN 2616-0684 (Print)
ISSN 2616-0692 (Electronic)

contributions of the compounds to the overall inhibition efficiency of the extract.

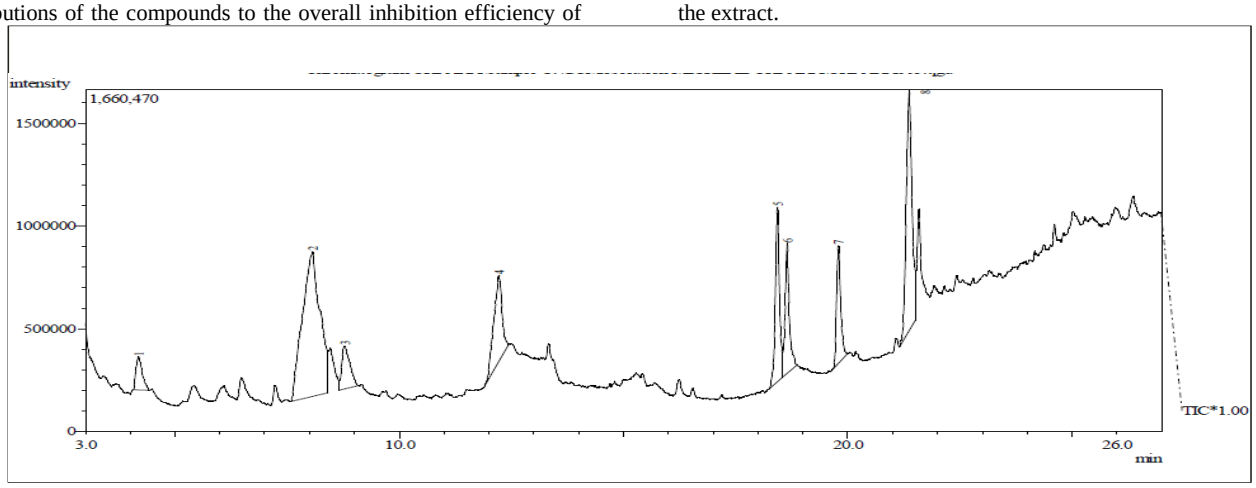

Figure 1: GCMS of the seed extracts of *Buchholzia coriacea* seed

Table 1: GC-MS data of ethanol extract of *Bucholzia coriacea* seed

Peak Number	Retention Time	Name of Compound	Molecular Formula	Molecular Weight	Peak area %
1	4.189	4,5-Dihydro-2-methylimidazole-4-one	$C_4H_6N_2O_8$	98	3.79
2	8.067	4,6-Dimethyltetrahydro-2H-pyran-2-one	$C_7H_{12}O_2$	128	3.02
3	8.782	1-Methyl-pyrrolidine-2-carboxylic acid	$C_6H_{11}NO_2$	129	3.64
4	12.226	2-Pyrrolidinoethylamine	$C_6H_{14}N_2$	114	4.69
5	18.434	(4E)-4-Methyl-4-hepten-3-one	$C_8H_{14}O$	126	23.42
6	18.665	Nitro-isobutyl glycerol	$C_4H_9NO_5$	151	10.51
7	19.794	1,4-Dimethoxy-2-methylcyclohexane	$C_9H_{18}O_2$	158	47.14
8	21.374	1-Pentadecanecarboxylic acid	$C_{16}H_{32}O_2$	256	3.79

However, this can only be qualitative since the individual contributions cannot be ascertained. The reason for the high inhibition efficiency obtained with biomass additives is that every component contributes to the total value.

In a corrosion system containing inhibitor, the inhibitor and the metal act as a Lewis base and a Lewis acid, respectively, therefore the frontier orbital theory may be used to determine possible modes of interaction between the inhibitor and metal. The frontier orbital energies E_{HOMO} and E_{LUMO}, can be related to the ionization potential, *I* and the electron affinity, *A*, of iron and the inhibitor molecule according to the Koopman's theorem: [28]

$$I = -E_{HOMO} \quad (2)$$

$$A = -E_{LUMO} \quad (3)$$

Absolute electronegativity χ and the absolute hardness, η, of the inhibitor are given by the equations below:[28]

$$\chi = \frac{(I + A)}{2} \quad (4)$$

$$\eta = \frac{(I - A)}{2} \quad (5)$$

The softness is the inverse of the hardness:

$$\sigma = \frac{1}{\eta} \quad (6)$$

The fraction of the electrons transferred from the inhibitor to the mild steel atom has the following relation:[34-36]

$$\Delta N = \frac{\chi_{Fe} - \chi_{inh}}{2(\eta_{Fe} + \eta_{inh})} \quad (7)$$

Where a theoretical electronegativity value of χ_{Fe} = 7.0 eV is taken for iron and absolute hardness of η_{Fe} = 0 is assumed, since *I* = *A* for bulk metals. The values of *A*, *I*, χ_{inh}, ΔN are given in Table 4. These values are comparable to those obtained by Rodriguez-Valdez *et al*. (2006)[25] for imidazolines inhibitors

Molecular dynamic simulations

To illustrate the adsorption progress of BCS extract on the metal surface at the molecular level involved performing a molecular dynamics simulation in a Forcite module available in the MS Modeling 4.0 software to sample many different low-energy configurations to identify the low energy minima.[15, 23] The calculations involved an 8 x 8 supercell, Fe crystal cleaved along the (1 1 0) plane, a COMPASS force field and the Smart algorithm; NVE (microcanonical) ensemble. With temperature at 350 K, a time step time of and simulation time of 1fs and 5 ps respectively. The system was quenched every 250 steps. Optimized structures of DMM, DTP, MPC and PEA, and the Fe surface were the platform for the simulation, and the structures selected based on the availability of some special features such as heteroatoms and or pi electrons and double bonds. Using the quench molecular dynamics method above, we found the preferred binding sites for the molecules on the Fe surface and calculated the binding energy. Figure 3 shows the optimized (lowest-energy) adsorption models for single molecules of DMM, DTP, MPC, and PEA, respectively, on the Fe (110) surface from the simulation; solvent and charge effects were neglected. The molecules maintained a flat-lying adsorption orientation on the Fe surface, using the regions of high HOMO density acting as the adsorption sites. The binding energy (E_{Bind}) between each molecule and the Fe surface was calculated using equation 8: [34]

$$E_{Bind} = E_{Total} - (E_{Inh} + E_{Fe}) \quad (8)$$

Where the $E_{total}, E_{Inh} and\ E_{Fe}$ denote the total energy of the system, the inhibitor molecule and the metal surface respectively. In each case, the potential energies taken were the average of the five structures of lowest energy. The obtained values were -62.39 kcal/mol, 90.97 kcal/mol, -77.24 kcal/mol and -72.83kcal/mol for DMM, DTP, MPC and PEA, respectively. The binding

energies showed no significant difference between them except for DTP showing equal contribution to the overall inhibition efficiency.

Table 2: The Structure and nature of the predominant compounds

S/N	Name of the Compound	Structure of compound	Nature
1	4,5-Dihydro-2-methylimidazole-4-one (DMM)	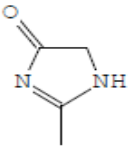	Ketone Compound
2	4,6-Dimethyltetrahydro-2H-pyran-2-one (DTP)	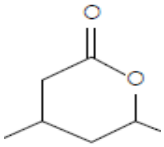	Ketone Compound
3	1-Methyl-pyrrolidine-2-carboxylic acid (MPC)	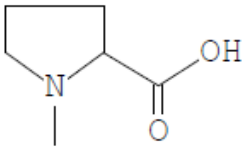	Alkaloid
4	2-Pyrrolidinoethylamine (PEA)	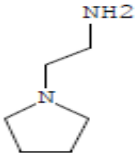	Alkaloid
5	(4E)-4-Methyl-4-hepten-3-one (MHT)	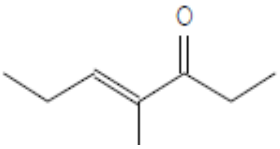	Ketone compound
6	Nitroisobutylglycerol (NBG)	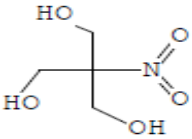	alcohol compound
`7	1,4-Dimethoxy-2-methylcyclohexane (DMH)	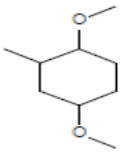	Ether compound
8	1-Pentadecanecarboxylic acid (PCA)	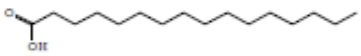	Fatty acid compound

Table 3: Molecular properties of compounds 1-8 calculated with Dmol3 module in the gas phase

Molecules	E_{Tot} (amu)	HOMO (eV)	LUMO (eV)	ΔE (eV)	μ (Debye)	ΔE/2
DMM	-337.895	-6.492	-1.081	5.411	6.9112	2.71
DTP	-420.908	-5.973	-0.904	5.069	4.9067	2.53
MPC	-436.848	-6.811	-1.578	5.233	3.5877	2.62
PEA	-343.517	-6.492	-1.339	5.153	0.4895	2.58
MHT	-385.113	-7.397	-2.247	5.150	3.2399	2.58
NBG	-584.294	-6.580	-1.455	4.125	3.3014	2.57
DMH	-499.939	-5.498	-0.616	4.882	2.9859	3.06
PCA	-811.453	-5.714	-1.285	4.429	4.2958	2.22

Adsorption isotherm

An adsorption isotherm can clarify the adsorptive conduct of an inhibitor. Langmuir, Frumkin, Temkin and Freundlich isotherms were the most considerably utilized adsorption isotherm.[37] In order to correlate the molecular modeling results with the inhibitory action of BC extract; weight loss data was applied to the various adsorption

ISSN 2616-0684 (Print)
ISSN 2616-0692 (Electronic)

isotherms, with the Langmuir giving the best fit (Figure 4). The applicability of the Langmuir isotherm implies that the mode of inhibitory action is, indeed, adsorption. Table 5 shows the corrosion rate (C_R) for various inhibitor concentrations (C_{inh}), inhibition efficiency (IE%) as well as the surface coverage by the inhibitor, θ, calculated from IE/100.

Effect of temperature

Equation 9 gives the Arrhenius equation as used to explore the temperature dependence of the corrosion reaction and the activation energy of the process:

$$CR = A\left(-\frac{E_a}{RT}\right) \quad (9)$$

where C_R is the corrosion rate, A is the Arrhenius pre-exponential constant, R is the universal gas constant and T, the absolute temperature. Plotting the natural logarithm of the corrosion rate versus 1/T (Figure 5), the activation energy can be calculated from the slope. The respective effective energies of activation obtained were 16.27, 17.81 and 19.05 kJ/mol for the uninhibited and containing 50 and 100 mg/L respectively. The increase of the activation energy in the inhibited systems indicates preferential physical bonding of the inhibitor molecules to the metal surface.

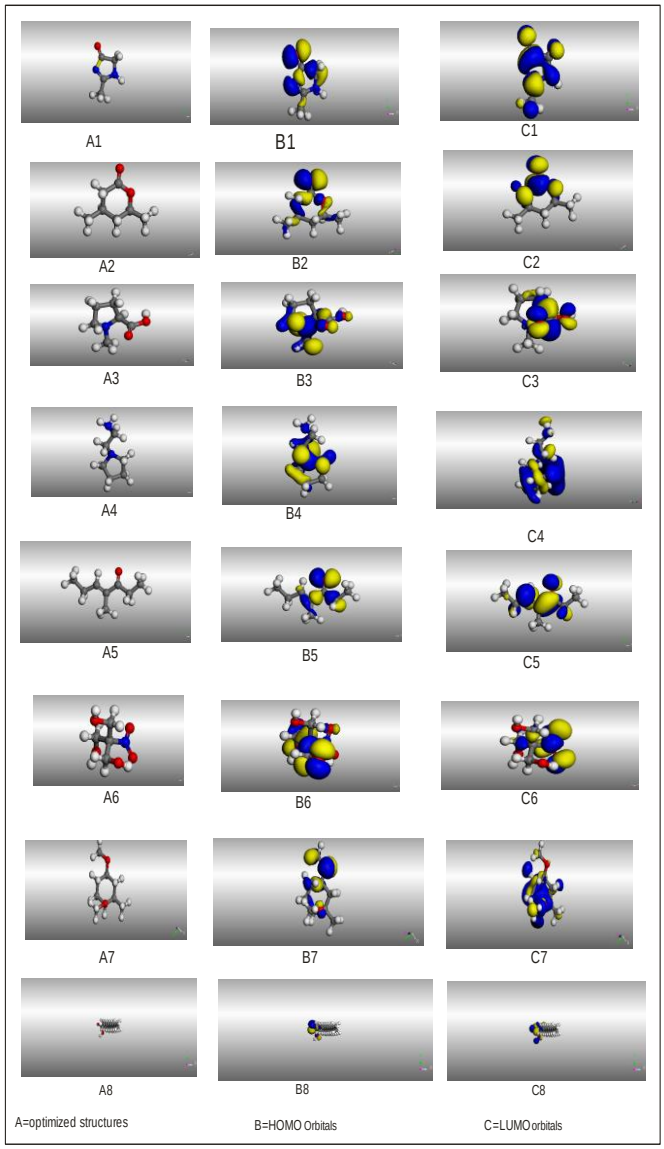

Figure 2: Optimized structures of the 8 BCS extracts, DMM, DTP, MPC, PEA, MHT, NBG, DMH and PCA; A = the optimized structures, B = the HOMO orbitals and C = the LUMO orbitals.

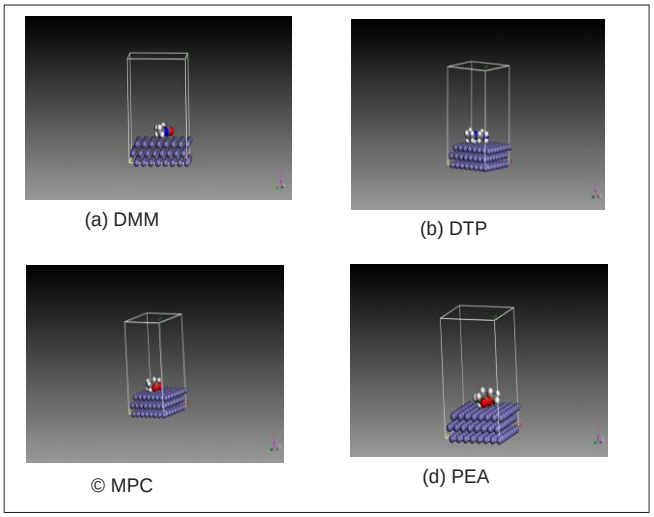

Figure 3: Molecular dynamics model of the adsorption of single molecules of: **(a)** DMM **(b)** DTP, **(c)** MPC and **(d)** PEA on Fe (1 1 0) surface.

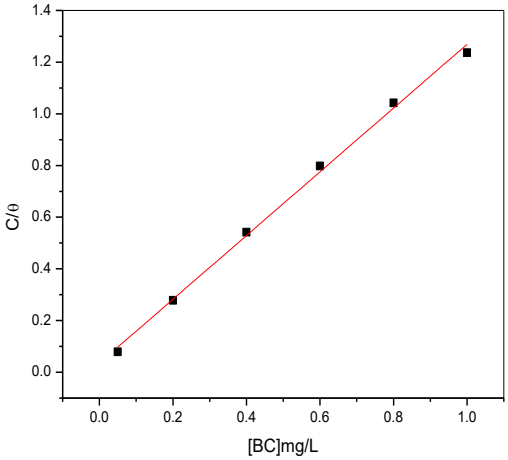

Figure 4: Langmuir adsorption isotherm fitted to the experimental surface coverage of mild steel by BC extracts components in 1M HCl. Correlation coefficient equals 0.99877.

Table 4: Absolute electronegativity, $\chi_{(eV)}$ and absolute hardness, $\eta_{(eV)}$ and the number of electrons, ΔN transferred between the eight BCS extract compounds and the iron surface.

ISSN 2616-0684 (Print)
ISSN 2616-0692 (Electronic)

Compound	$\chi(eV)$	$\eta(eV)$	ΔN
DMM	3.79	2.71	0.59
DTP	3.44	2.54	0.70
MPC	4.20	2.62	0.53
PEA	3.92	2.58	0.60
MHT	4.82	2.58	0.42
NBG	4.02	2.56	0.58
DMH	3.06	2.44	0.81
PCA	3.50	2.22	0.74

Table 5: Weight loss parameters for mild steel corrosion inhibition in 1 M HCl containing various concentration of BCS extract at 303K for 24hrs

Inhibitor Concentration loss (mg/L)	Weight (mg)	Corrosion Rate (mg/cm^2-h)	Inhibition Efficiency (IE%)
Blank	159.90	0.2177	0
50	38.50	0.0840	63.26
200	29.40	0.0641	71.95
400	27.50	0.0600	73.76
600	26.00	0.0567	75.17
800	21.30	0.0465	76.81
1000	20.00	0.0436	80.91

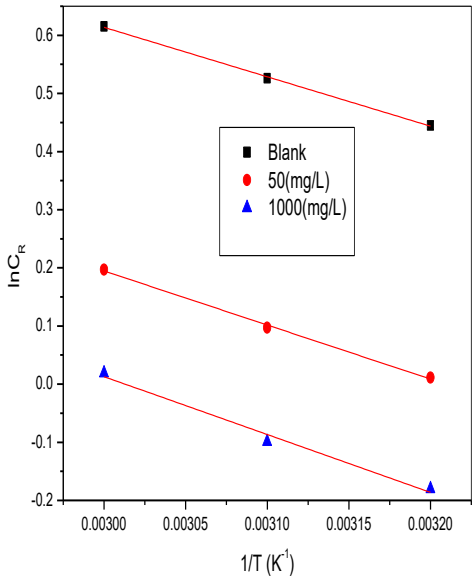

Figure 5: Plot of Arrhenius equation for $\ln C_R$ against T^{-1} for mild steel corrosion in presence and absence of BC

Conclusion

The possibility of using *Bucholzea coriacea seed* (BCS) extract as a corrosion inhibitor for mild steel in 1 M HCl has been explored. Results obtained showed that ethanol extract of BCS is a good green corrosion inhibitor, with its efficiency increasing as the inhibitor concentration increased reaching its highest value with the addition of 1000 mg/L. The adsorption of BCS extract on mild steel surface in 1 M HCl solution obeyed the Langmuir isotherm. Moreover, the calculated thermodynamic energy of activation (Ea) indicated that the extract adsorbed on the mild steel by a physisorption-based mechanism. The theoretical study on active principles identified in this extract indicate similar capacity for charge donation. The negative value of the binding energy is an indication of strong adsorption of the compounds on the mild steel surface. The theoretical modeling calculations results, together with those obtained from the adsorption theory, gave a consistent view of the corrosion system investigated.

Conflict of Interest

The authors declare no conflict of interest.

Authors' Declaration

The authors hereby declare that the work presented in this article is original and that any liability for claims relating to the content of this article will be borne by them.

Acknowledgements

The authors acknowledge Electrochemical and Material Research Unit (EMRU) of the Department of Chemistry in providing its facilities for conducting the study and The African Centre of Excellence in Future Energies and Electrochemical Systems (ACE-FUELS) in providing technical assistance

References

1. Akalezi CO, Maduabuchi CA, Enenebeaku CK, Oguzie EE. Experimental and DFT evaluation of adsorption and inhibitive properties of *Moringa oliefera* extract on mild steel corrosion in acidic media. Arab J Chem. 2020; 13:9270-9282.
2. Jafari H, Akbarzade K, Danaee I. Corrosion inhibition of carbon steel immersed in a 1 M HCl solution using benzothiazole derivatives. Arab J Chem. 2019; 12:1387-1394.
3. Al-Baghdadi BA, Hashim FG, Salam AQ, Abed TK, Gaaz TS, Al-Amiery AA, Kadhum AAH, Reda KS, Ahmed WK. Synthesis and corrosion inhibition application of NATN on mild steel surface in acidic media complemented with DFT studies. Results Phys. 2018; 8:1178-1184.
4. Fadare OO, Okoronkwo AE, Olasehinde EF. Assessment of anti-corrosion potentials of extract of *Ficus asperifolia* -Miq (Moraceae) on mild steel in acidic medium. Afr J Pure Appl Chem. 2016; 10(1):8-22.
5. Geethamani P and Kasthuri PK. The inhibitory action of expired asthalin drug on the corrosion of mild steel in acidic media: A comparative study. J Tiawan Inst Chem Eng. 2016; 63:490-499.
6. Loto RT, Popoola AP, Olaita AL. Synergistic effect of P-phenylenediamine and n,n-diphenylthiourea on the electrochemical corrosion behaviour of mild steel in dilute acid media. Int J Ind Chem. 2016; 7:143-155.
7. Jalajaa D, Jyothi S, Muruganantham VR, Mallika J. *Moringa Oleifera* gum exudate as corrosion inhibitor on mild steel in acidic medium. Rasayan J Chem. 2019; 12(2):545-548.
8. Torres AR, Valladares Cisneros MG, González Rodríguez JG. *Medicago sativa* as a green corrosion inhibitor for 1018 carbon steel in 0.5 M H_2SO_4 solution. Green Chem Lett Rev. 2016; 9(3):143-155
9. Maduabuch CA, Njoku DI, Obike IA, Simeon C, Nwanonenyi SC, Akalezi CO, Adindu BC, Oguzie EE. Experimental and Theoretical Studies on the Protective Effect of a Biomass Corrosion Inhibitor (*vigna radiata)* on Mild Steel in Acidic Medium. Electroanalysis. 2020; 32:3117-3130
10. Oguzie EE, Iheabunike ZO, Oguzie KL, Ogukwe CE, Chidiebere MA, Enenebeaku CK, Akalezi CO. Corrosion Inhibiting Effect of *Aframomum melegueta* Extracts and Adsorption Characteristics of the Active Constituents on Mild

Steel in Acidic Media. J Dispers Sci Technol. 2013; 34(4):516-527.
11. Arthur DE and Abechi SE. Corrosion inhibition studies of mild steel using *Acalypha chamaedrifolia* leaves extract in hydrochloric acid medium. SN Applied Sci. 2019; 1(9):1-11.
12. Omar B, Chaouki S, Salghi R. Inhibition of acid corrosion of mild steel by *Anacyclus pyrethrum* L. Extracts. Res Chem Intermed. 2014; 40:259-268.
13. Verma C, Ebenso EE, Quraishi MA. Alkaloids as green and environmental benign corrosion inhibitors: An overview. Int J Corr Scale Inhib. 2019; 8(3):512-528.
14. Loto RT. Corrosion inhibition effect of non-toxic-amino acid compound on high carbon steel in low mola concentration of hydrochloric acid. J Mater Res Technol. 2019; 8(1):484-493.
15. Oguzie EE, Enenebeaku CK, Akalezi CO, Okoro SC, Ayuk AA, Ejike EN. Adsorption and corrosion-inhibiting effect of *Dacryodis edulis* extract on low-carbon-steel corrosion in acidic media. J Coll Interf Sci. 2010; 349(1):283-292.
16. Izah SC, Uhunmwangho EJ, Eledo BO. Medicinal potentials of *Buchholzia coriacea* (wonderful kola). J Med Plant Res. 2018; 8(5):27-42.
17. Malomo RO, Bankole OE, Sorinola AO. Phytochemical and Chemical Properties of Raw, Cooked and Dried Seeds of *Buchholzia coriacea*. J Sci Res. 2017; 16(4):1-8.
18. Enechi OC, Okeke ES, Nwankwo NE, Abonyi CU, Ugwu L, Eze P, Agbo NC, Enwerem UC. Phytochemical Screening and evaluation of the anti-inflammatory effect of flavonoid-rich seed extract of *Buchholzia coriacea* in rats. Indo Am J Pharm. 2019; 6(8):15525-15534.
19. Abubakar A, Jigam AA, Kabir AY, Adefolaju OV. Phytochemical Constituents and *In Vitro* Anti-trypanosomal Activity of Ethanol Seed Extract of *Buchholzia Coriacea*. J Pure Appl Sci. 2017; 4:43-48.
20. Ezeigbo OR, Ejike EN, Nwachukwu I, Ejike BU. Comparatie antibacterial activity of methanolic, ethanolic and aqueous extract of Garcinia kola (bitter kola) and *Cola nitida* (Kola nut). Int J Plant Res. 2016; 6(3):53-56.
21. Umeokoli BO, Abba C, Ezeh P, Ajaghaku D. Antimicrobial, anti-inflammatory, and chemical evaluation of *Buchholzia coriacea* seed (Wonderful kola). Am J Life Sci. 2016; 4(5):106-112.
22. Vorobyova1 V, Chygyrynets O, Skiba M, Overchenko T. Experimental and theoretical investigations of anti-corrosive properties of thymol. Chem Chem Technol. 2019; 13(2):261-268.
23. Akalezi CO, Enenebaku CK, Oguzie EE. Application of aqueous extracts of coffee senna for control of mild steel corrosion in acidic environments. Int J Ind Chem. 2012; 3(13):1-12.
24. Perdew JP, Burke K, Ernzerhol. Generalized Gradient approximation Made Simple, Phys Rev Lett. 1996; 77(18):3865-3868.
25. Rodrıguez-Valdez LM, Villamisar W, Casales M, Gonza´lez-Rodriguez JG, Alberto, Martınez-Villafane A, Martinez L, Glossman-Mitni D. Computational simulations of the molecular structure and corrosion properties of amidoethyl, aminoethyl and hydroxyethylimidazolines inhibitors. Corros Sci. 2006; 48:4053-4064.
26. Ju H, Ka ZPi, Li Y. Aminic nitrogen-bearing polydentate Schiff base compounds as corrosion inhibitors for iron in acidic media: a quantum chemical calculation, Corros Sci. 2008; 50:865-871.
27. Zhao P, Liang Q, Li Y. Electrochemical, SEM/EDS and quantum chemical study of phthalocyanines as corrosion inhibitors for mild steel in 1M HCl. Appl Surf Sci. 2005; 252:1596-1607.
28. Sastri VS and Perumarredi JR. Molecular orbital theoretical studies of some organic corrosion inhibitors. Corrosion. 1997; 53(8):617-622.
29. Akalezi1 CO, Ogukwe CE, Enenebaku1 CK, Oguzie EE. Corrosion Inhibition of Aluminium Pigments in Aqueous Alkaline Medium Using Plant Extracts. Environ Pollut. 2012; 1(2):45-60.
30. Rodríguez-Valdez ML, Martínez-Villafañe A, Glossman-Mitnik DJ. Computational simulation of the molecular structure and properties of heterocyclic organic compounds with possible corrosion inhibition properties. Mol Struct (Theochem). 2005; 713:65-70.
31. Ahmed M. Al-Sabagh, Notaila M. Nasser, Ahmed A. Farag, Mohamed A. Migahed, Abdelmonem MF. Eissa, Tahany Mahmoud, Structure effect of some amine derivatives on corrosion inhibition efficiency for carbon steel in acidic media using electrochemical and Quantum Theory Methods. Egy J Pet. 2013; 22:101-116.
32. Benali O, Larabi L, Traisnel M, Gengembre L, Harek Y. Electrochemical, theoretical and XPS studies of 2-mercapto-1-methylimidazole adsorption on carbon steel 1M $HClO_4$. Appl Surf Sci. 2007; 253(14):6130-6139.
33. Jianhong Tan, Lei Guo, Hong Yang, Fan Zhangc and Youness ElL- Bakri, Synergistic effect of potassium iodide and sodium dodecyl sulfonate on the corrosion inhibition of carbon steel in HCl medium: a combined experimental and theoretical investigation. RSC Adv. 2020; 10:15163.
34. Martinez S and Stagljar I. Correlation between molecular structure and the corrosion inhibition efficiency of chestnut tannin in acidic solutions. J Mol Struc-Theochem. 2003; (640):167-174.
35. Klopman G. Chemical reactivity and the concept of charge- and frontier-controlled reactions. J Am Chem Soc. 1968; 90:223-234.
36. Bartley J, Huynh N, Bottle SE, Flitt H, Notoya T, Schweinsberg DP. Computer simulation of the corrosion inhibition of copper in acidic solution by alkyl esters of 5-carboxybenzotriazole, Corros Sci. 2003; 45:81-96.
37. Diki NYS, Coulibaly NH, Yao TNS, Trokourey A. Thermodynamic and DFT studies on the behavior of cefadroxil drug as effective corrosion inhibitor of copper in one molar nitric acid medium. J Mater Environ Sci. 2019, 10(10):926-938.